

Elastic e-p scattering at ePIC for Early Physics

M. Osipenko
INFN sez. di Genova

ePIC and EIC Physics Readiness Workshop, Cosenza, 18 March 2026

Early science data

- for elastic scattering only e-p runs will be considered, years 2 and 3 will provide overall data amount of about 10 fb^{-1} for this study;
- year 4 will provide 8 fb^{-1} at higher energy, which are less interesting due to lower p' acceptance in FD:

$$\theta_p \xrightarrow{E \rightarrow \infty} \frac{\sqrt{Q^2}}{E_p}$$

→ per nucleon

	Species	Energy (GeV)	Luminosity/year (fb ⁻¹)	Electron polarization	p/A polarization
YEAR 1	e+Ru or e+Cu	10 x 115	0.9	NO (Commissioning)	N/A
YEAR 2	e+D e+p	10 x 130 ★	11.4 4.95 - 5.33	LONG	NO TRANS
YEAR 3	e+p	10 x 130 ★	4.95 - 5.33	LONG	TRANS and/or LONG
YEAR 4	e+Au e+p	10 x 100 10 x 250 ★	0.84 6.19 - 9.18	LONG	N/A TRANS and/or LONG
YEAR 5	e+Au e+ ³ He	10 x 100 10 x 166	0.84 8.65	LONG	N/A TRANS and/or LONG

Note: the eA luminosity is per nucleon

- e+D and e+³He runs could be used to access neutron form-factors, but require a different reconstruction procedure: LFHCAL + B0 EmCal (mixed with γ).

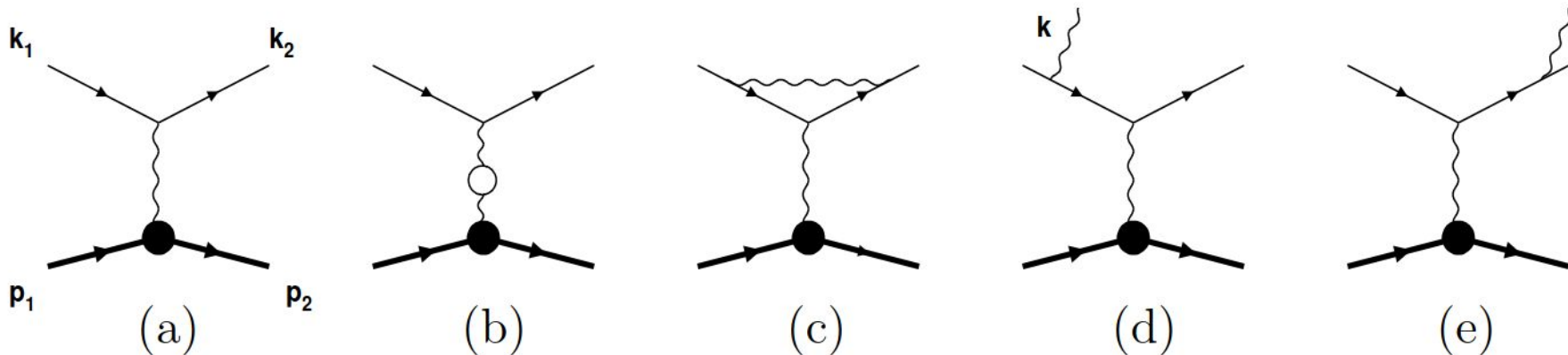
Elastic e-p scattering

- the process under study is 2→2 type:

$$e(k) + p(P) \rightarrow e'(k') + p'(P')$$

- QED Radiative Corrections to this process change the peak value and add the bremsstrahlung tail;
- cross section/polarization asymmetries give access to proton EM-form-factors $G_E(Q^2)$ and $G_M(Q^2)$:

$$\frac{d\sigma}{dQ^2} \approx \frac{4\pi\alpha^2}{Q^4} \left[\frac{G_E^2 + \tau G_M^2}{1 + \tau} \right] \quad \text{for } s \gg Q^2, M^2$$



Target (proton) polarization asymmetry

- scattering off a polarized proton gives asymmetry [[C.F. Perdrisat et al., Prog. Part. Nucl. Phys. 59, \(2007\) 694](#)] in TRF:

$$A = -\frac{2\sqrt{\tau(1+\tau)} \tan(\theta_e/2)}{G_E^2 + \frac{\tau}{\epsilon} G_M^2} \left[\sin \theta^* \cos \phi^* G_E G_M + \sqrt{\tau[1 + (1+\tau) \tan^2(\theta_e/2)]} \cos \theta^* G_M^2 \right]$$

- for target polarized transversely to q we obtain Target Spin Asymmetry:

$$\langle \cos \phi^* \rangle \sim \frac{G_E G_M}{G_E^2 + \frac{\tau}{\epsilon} G_M^2} \sim \frac{G_E}{G_M}$$

- in collider kinematics invariant form should be used [[A. Afanasev et al., Phys. Rev. D 64 \(2001\) 113009](#)]:

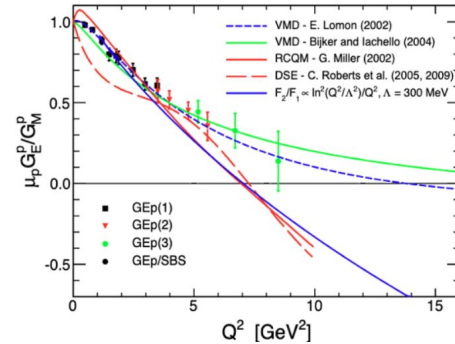
$$\frac{d\sigma_0}{dQ^2} = \frac{2\pi\alpha^2}{S^2 Q^4} \sum_i \theta_B^i \mathcal{F}_i \quad \mathcal{F}_3 = -2M^2 G_E G_M, \quad \mathcal{F}_4 = -M^2 G_M \frac{G_E - G_M}{1 + \tau_p}$$

$$\theta_3^B = \frac{2m}{M} (q \eta k_2 \xi - \eta \xi Q^2),$$

$$\theta_4^B = \frac{m Q^2 q \eta}{M^3} (2p_1 \xi - k_2 \xi),$$

$$\eta_L = \frac{1}{\sqrt{\lambda_s} \lambda} \left(k_1 - \frac{S}{M} p_1 \right),$$

$$\eta_T = \frac{1}{\sqrt{\lambda_s} \lambda} [(-SX + 2M^2 Q^2 + 4m^2 M^2) k_1 + \lambda_s k_2 - (SQ^2 + 2m^2 S_x) p_1],$$



- in collider kinematics invariant form should be used [[A. Afanasev et al., Phys. Rev. D 64 \(2001\) 113009](#)]:

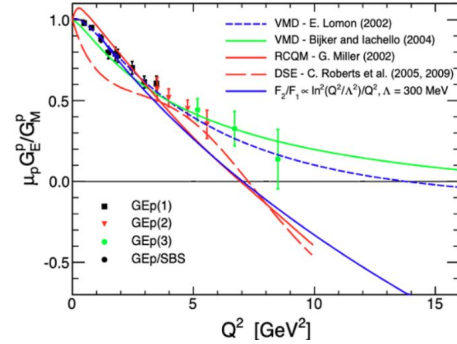
Double polarization asymmetry

- longitudinal polarization of electrons and protons in elastic scattering gives double spin asymmetry [[M.J. Alguard et al., Phys.Rev.Lett.37, 1258 \(1976\)](#)] in TRF:

$$A_{LL} = 2\tau \frac{G_M \frac{M}{E} + \frac{G_M}{G_E} [\tau \frac{M}{E} + (1 + \tau) \tan^2 \frac{\theta}{2}]}{G_E \left(1 + \frac{\tau}{\epsilon} \left(\frac{G_M}{G_E} \right)^2 \right)} \xrightarrow{E \rightarrow \infty} \frac{2\tau}{\frac{\tau}{\epsilon} + \left(\frac{G_E}{G_M} \right)^2} (1 + \tau) \tan^2 \frac{\theta}{2}$$

- for not very large Q^2 the asymmetry may give access to the form-factor ratio (requires 1% precision);

$$\epsilon = \frac{1 - y}{1 - y - \frac{1}{2}y^2} \rightarrow 1 \quad \tau = \frac{Q^2}{4M^2} \quad A_{LL} \xrightarrow{Q^2 \rightarrow \infty} 2\epsilon\tau \left(\frac{M}{E} + \tan^2 \frac{\theta}{2} \right)$$



- in collider kinematics invariant form should be used [[A. Afanasev et al., Phys. Rev. D 64 \(2001\) 113009](#)]:

$$\frac{d\sigma_0}{dQ^2} = \frac{2\pi\alpha^2}{S^2 Q^4} \sum_i \theta_B^i \mathcal{F}_i \quad \mathcal{F}_3 = -2M^2 G_E G_M, \quad \mathcal{F}_4 = -M^2 G_M \frac{G_E - G_M}{1 + \tau_p}$$

$$\theta_3^B = \frac{2m}{M} (q \eta k_2 \xi - \eta \xi Q^2),$$

$$\eta_L = \frac{1}{\sqrt{\lambda_s}} \left(k_1 - \frac{S}{M} p_1 \right),$$

$$\theta_4^B = \frac{m Q^2 q \eta}{M^3} (2p_1 \xi - k_2 \xi),$$

$$\eta_T = \frac{1}{\sqrt{\lambda_s \lambda}} [(-SX + 2M^2 Q^2 + 4m^2 M^2) k_1 + \lambda_s k_2 - (SQ^2 + 2m^2 S_x) p_1],$$

Parity-violating Single Spin Asymmetry

- scattering of polarized electrons of an unpolarized proton allows to observe γ -Z interference:

$$\varepsilon' \equiv \sqrt{\tau(1+\tau)(1-\varepsilon^2)},$$

$$A_{ep}^{PV} \equiv \frac{\sigma_+ - \sigma_-}{\sigma_+ + \sigma_-} \approx \frac{2\Re(\mathcal{M}_{EM}\mathcal{M}_{\text{weak}})}{|\mathcal{M}_{EM}|^2 + \Re(\mathcal{M}_{EM}\mathcal{M}_{\text{weak}})}.$$

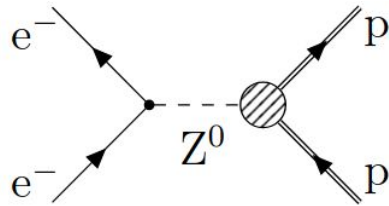
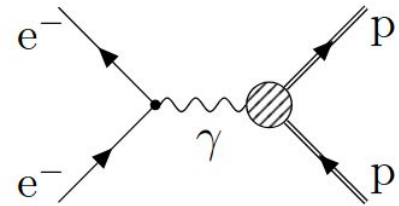
In the large energy limit we will get:

$$y = \frac{Q^2}{s} \rightarrow 0$$

$$\varepsilon = \frac{1-y}{1-y-\frac{1}{2}y^2} \rightarrow 1$$

$$A_{ep}^{PV} = \left(\frac{-G_F Q^2}{4\pi\alpha\sqrt{2}} \right) \left(\frac{\varepsilon G_E^\gamma G_E^Z + \tau G_M^\gamma G_M^Z + g_V^e \varepsilon' G_M^\gamma G_A^e}{\varepsilon (G_E^\gamma)^2 + \tau (G_M^\gamma)^2} \right),$$

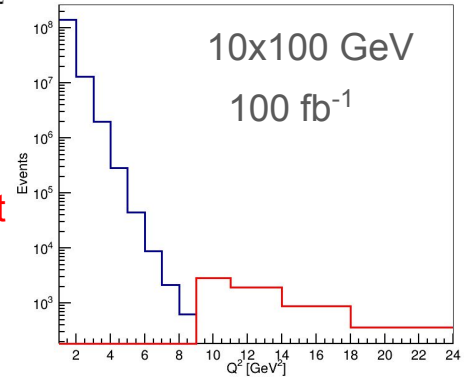
$$A_{ep}^{PV} \underset{Q^2 \rightarrow \infty}{\simeq} \left(-\frac{G_F Q^2}{4\pi\alpha\sqrt{2}} \right) \left[\frac{G_M^Z}{G_M^\gamma} + g_V^e y \frac{G_A^e}{G_M^\gamma} \right] \simeq \left(-\frac{G_F Q^2}{4\pi\alpha\sqrt{2}} \right) \frac{G_M^Z}{G_M^\gamma}$$



$$A_{ep}^{PV} \simeq 10^{-4} \times Q^2$$

$$N > \frac{10^8}{Q^4}$$

but $N_{ep} > 10^6$ required at $Q^2 = 10 \text{ GeV}^2$.



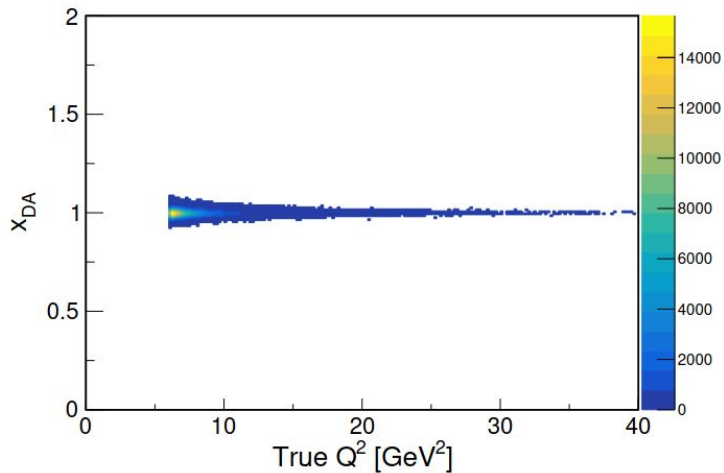
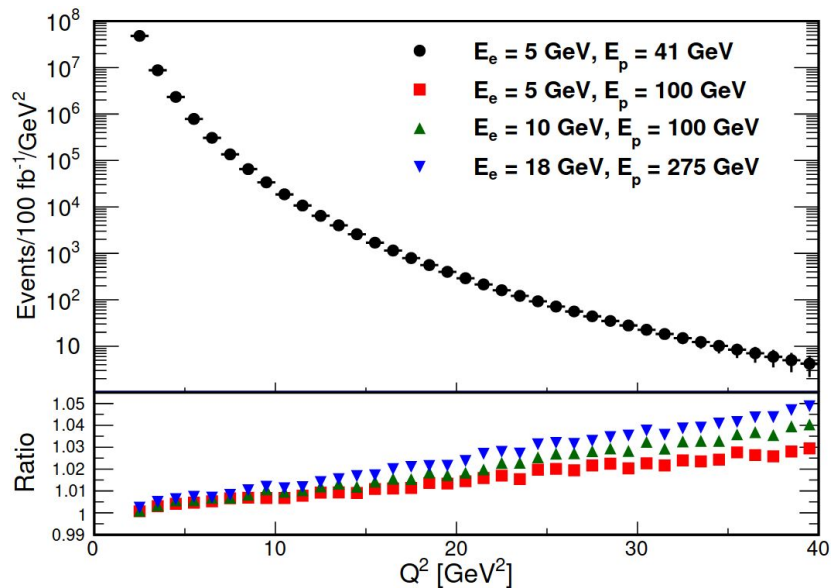
$$G_E^{\gamma,p} = \frac{2}{3}G_E^u - \frac{1}{3}G_E^d - \frac{1}{3}G_E^s$$

$$G_E^{Z,p} = \left(1 - \frac{8}{3}\sin^2\theta_W \right) G_E^u + \left(-1 + \frac{4}{3}\sin^2\theta_W \right) G_E^d + \left(-1 + \frac{4}{3}\sin^2\theta_W \right) G_E^s.$$

Previous study

B. Schmookler et al., [arxiv:2207.04378](https://arxiv.org/abs/2207.04378) (2022) + github.com + presentations:

- elastic cross sections can be obtained in range of $6 < Q^2 < 40 \text{ GeV}^2$;
- DA method allows to reconstruct x ;
- background can be removed by $\Delta\phi$, P_T , P_z and E cuts.



(d) DA method

Veto	Total Events (Scaled to 100 fb^{-1})
None	500×10^6 (8×10^{12})
1	148 (2.37×10^6)
1+2	1 (16000)
1+2+3	1 (16000)
1+2+3+4	0 (0)
1+2+3+4+5	0 (0)

This study

Generator:

- started with ELRADGEN 2.0 [I. Akushevich et al., Comput.Phys.Commun. 183 \(2012\) 1448-1467](#)
- adapted to high energy kinematics (few terms can still be improved);
- implemented of fully differential form in T Foam;
- calculation is completely Lorentz invariant - frame independent;
- include polarizations of both e^- and P beams;
- include both the elastic peak with radiative correction and hard bremsstrahlung tail;

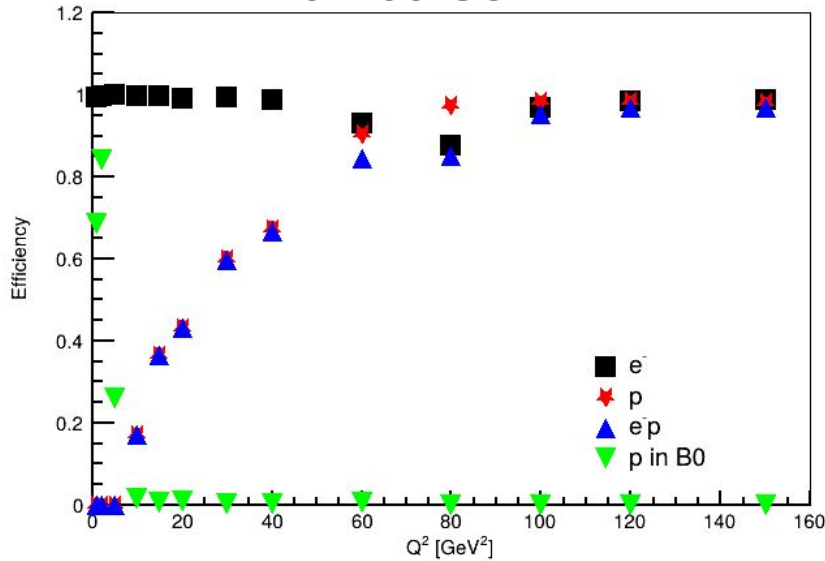
MC method:

- using beam effects through “abconv” v0.1.3 (approximate, changes energies);
- using “npsim” v1.4.6 simulations with the “epic_craterlake.xml” configuration;
- using “eicrecon” v2.4.3 reconstruction and root script to read results.

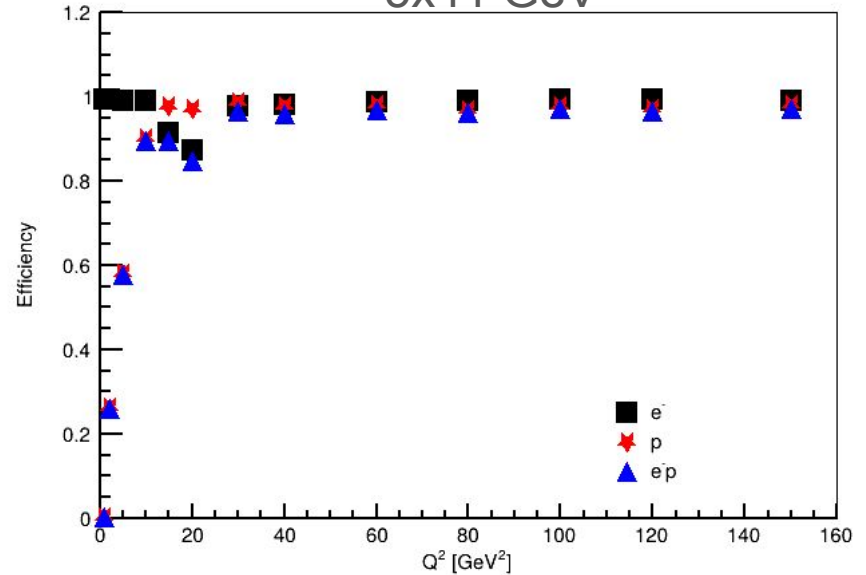
Elastic reaction efficiency

- efficiency is high for e^- everywhere, at least for $Q^2 > 1 \text{ GeV}^2$;
- for 10x100 GeV config. p-efficiency drops to zero at $Q^2 < 10 \text{ GeV}^2$ where p' goes into the gap between FD ($\eta < 3.5$) and B0 ($\eta > 4.6$) or in B0 (TruthSeeded tracking);
- for 5x41 GeV config. p-efficiency also falls at low Q^2 , and at $Q^2 = 1 \text{ GeV}^2$ it drops to 0.2%, while B0 efficiency is still negligible;

10x100 GeV

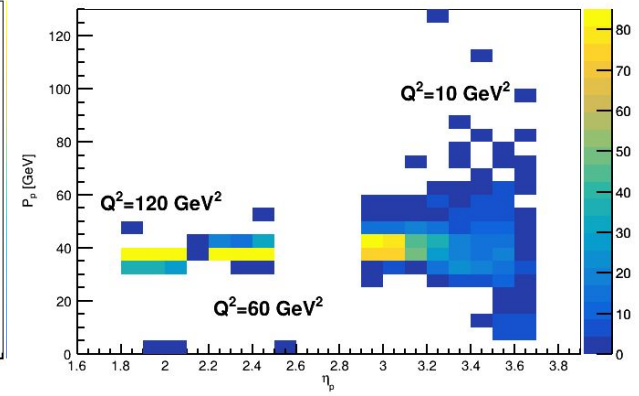
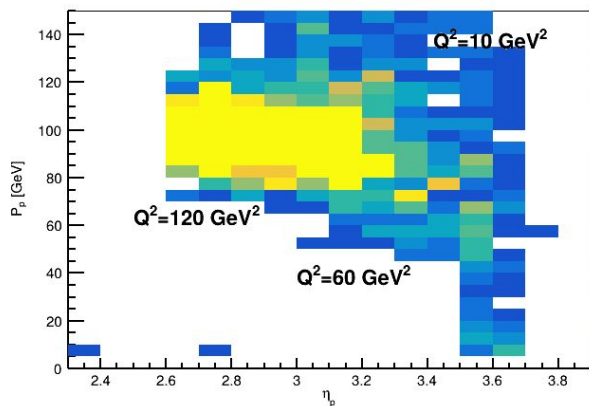
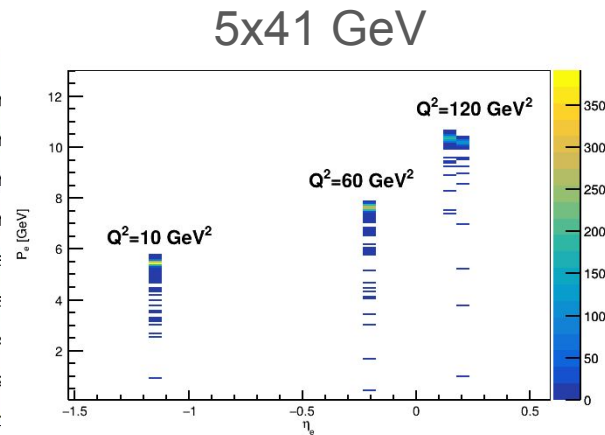
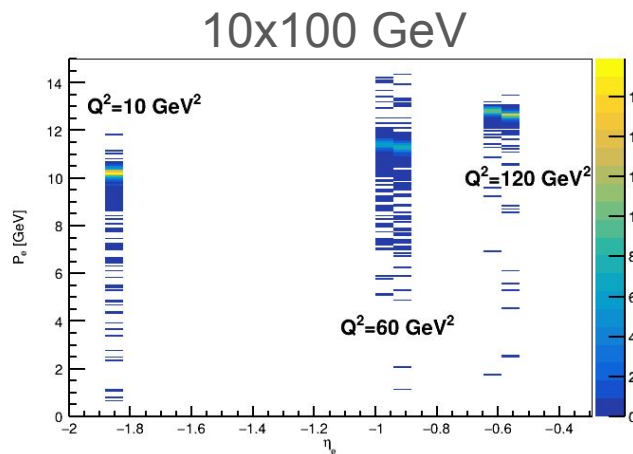


5x41 GeV



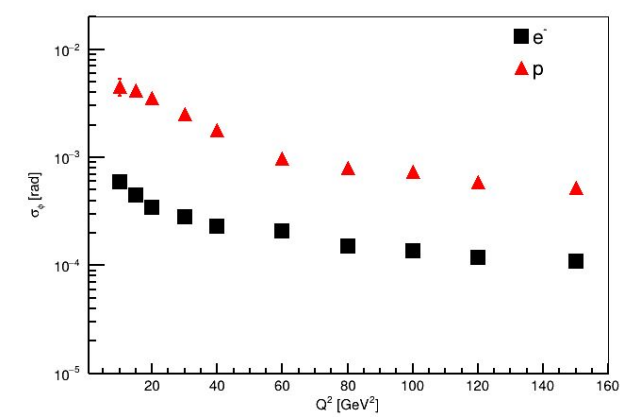
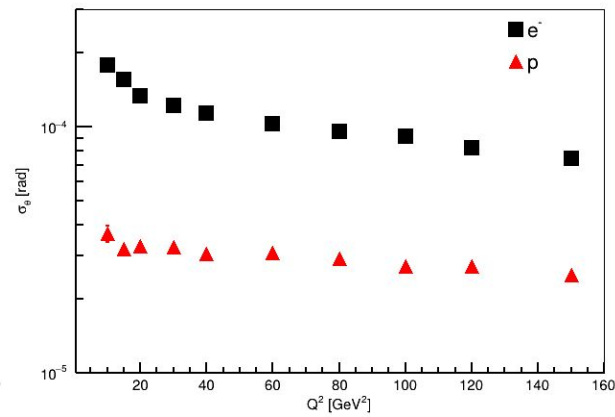
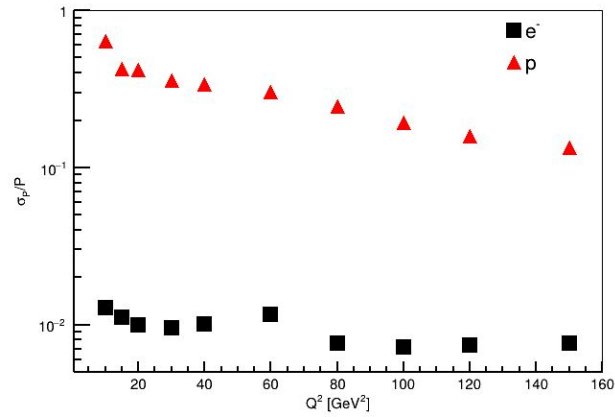
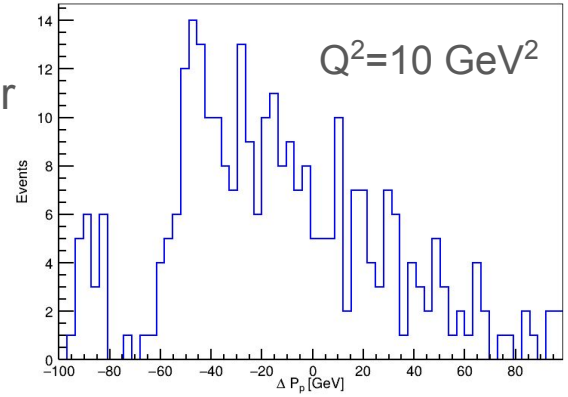
Elastic reaction kinematics

- e^- and p move with Q^2 into higher FD acceptance region, momenta remain almost fixed;
- at medium $Q^2=10-15 \text{ GeV}^2$ the proton sometimes goes into the detector gap: $3.5 < \eta < 4.6$;
- at low $Q^2=1-10 \text{ GeV}^2$ the proton goes into B0 $\eta > 4.6$;
- at $Q^2 < 0.1 \text{ GeV}^2$ the proton goes into RomanPots ($\eta > 6$);



Elastic reaction: particle resolutions

- e^- momentum and angular resolutions improve slightly with Q^2 ;
- p momentum and angular resolutions also improve with Q^2 ;
- e^- momentum resolution is better than p , opposite for angular resolutions;
- overall angular resolutions are good, while momentum resolution of proton is much larger than nucleon mass scale.



Momentum resolution of dRICH

- dRICH is measuring Cherenkov angle, assuming PID we can obtain particle momentum:

$$p = \frac{M}{\sqrt{(n^2 - 1) - n^2 \sin^2 \theta_C}}$$

- momentum resolution is then:

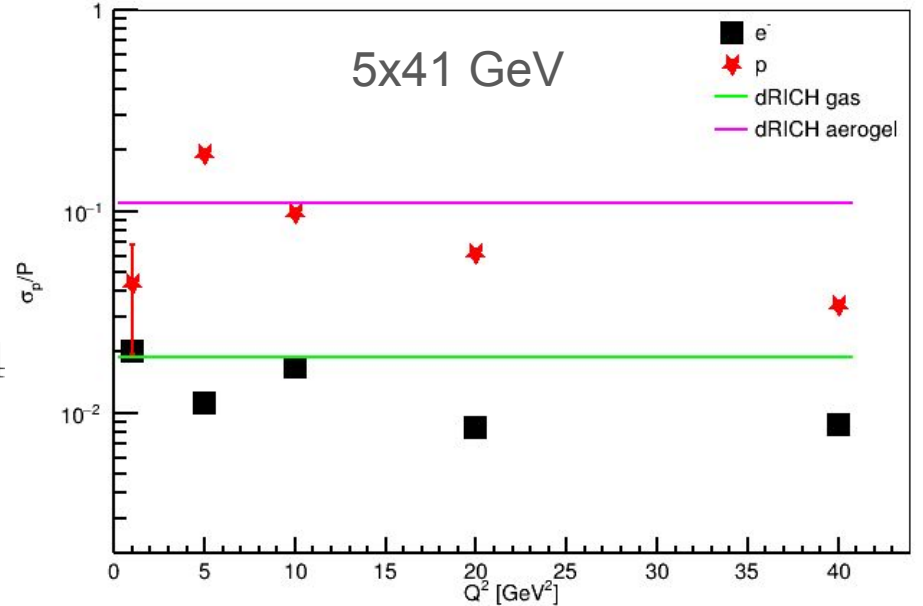
$$\frac{\sigma_p}{p} = n^2 \frac{p^2}{2M^2} \sin 2\theta_C \sigma_{\theta_C}$$

where:

$$\theta_C(gas) \sim 2^\circ \quad \sigma_{\theta_C} \sim 3 \times 10^{-4}$$

$$\theta_C(aerogel) \sim 11^\circ$$

better than tracking
(will not work for higher energies)

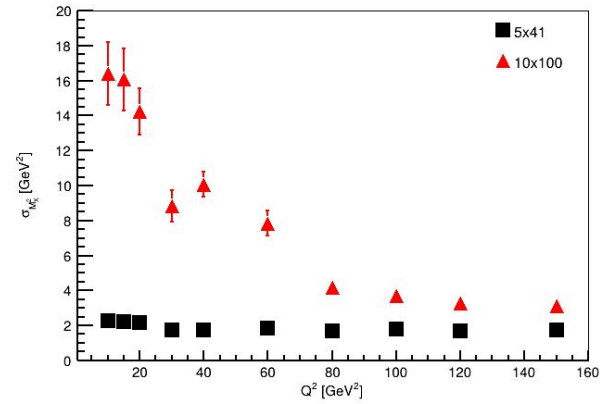
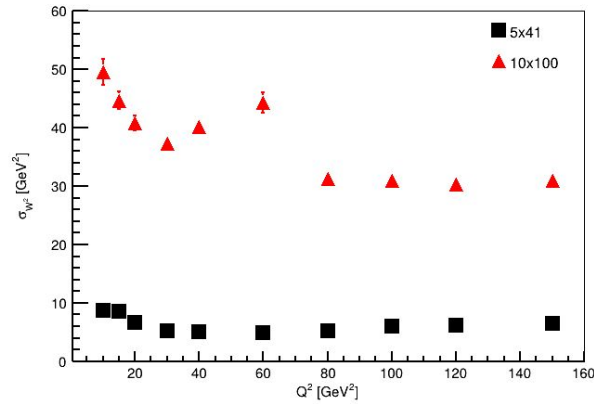
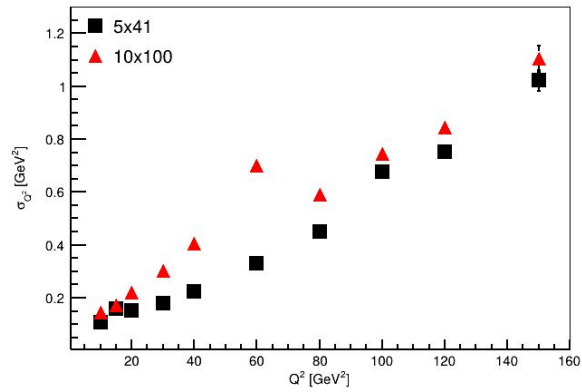


Elastic reaction: invariant resolutions

The measurement of elastic $e'p'$ cross section requires:

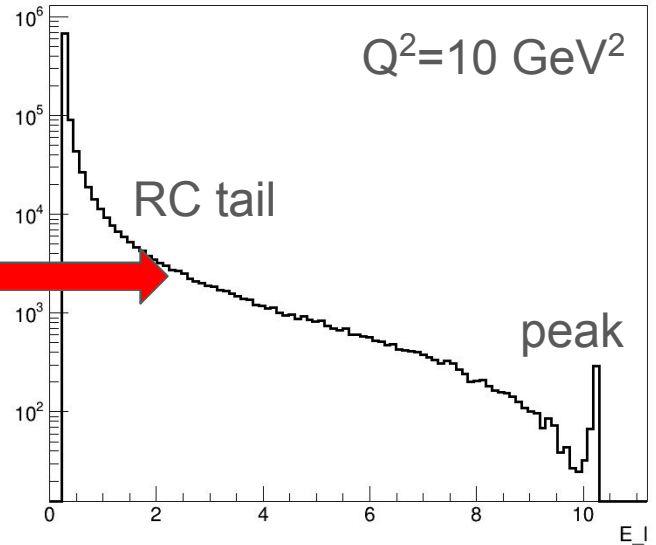
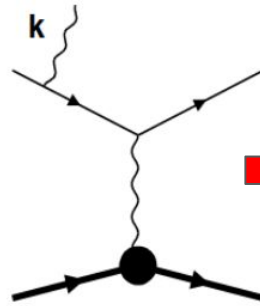
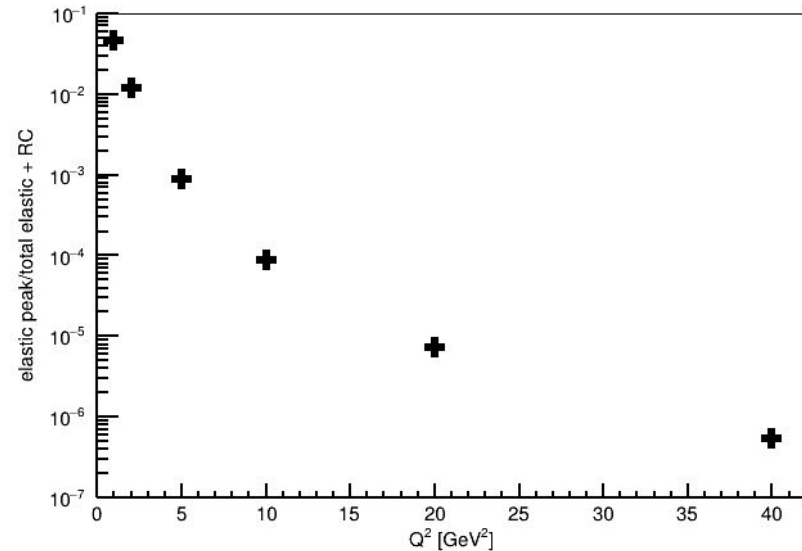
1. separation from radiative processes ($e'p'\gamma$) - $q+P$ invariant mass $< m_{\pi}$;
2. separation from inelastic processes ($e'p'X$) - $e+P$ missing mass $< m_{\pi}$ or momentum conservation veto;
3. reconstruction of the scale Q^2 .

Using directly reconstructed 4-momenta first two steps cannot be performed.



Elastic peak contribution

- NB at high Q^2 the contribution of the elastic peak into the total elastic cross section (including RC) becomes negligible;
- since bremsstrahlung gamma mass is zero the missing mass of this channel is also zero, the only separation can be done using electron W or x variables;
- to separate elastic peak ePIC must have W -resolution better than pion mass.



W^2 reconstruction

- q+P invariant mass is defined as following:

$$W^2 = (k + P - k')^2 = M^2 - Q^2 + y(s - M^2) \quad y = 1 - \frac{Pk'}{Pk}$$

- as noticed in previous study $y \sim 10^{-2}$ but its resolution is compromised by e' momentum resolution, however assuming that $2 \rightarrow 2$ process is already identified ($X=0$) it can be improved using p' angles:

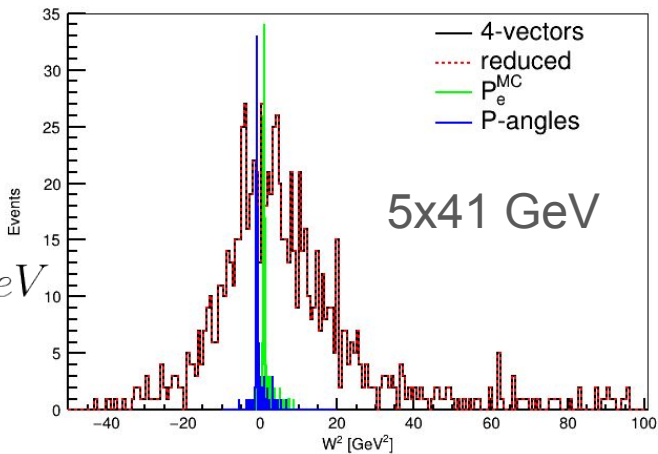
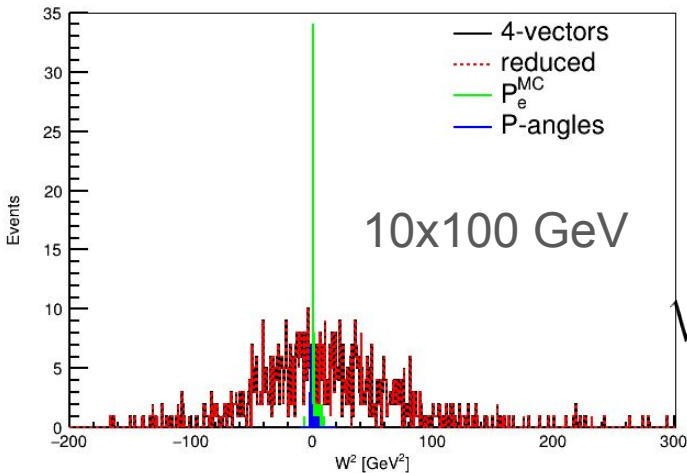
not working for collinear γ

$$y = \frac{PP' - M^2}{Pk}$$

$$|\vec{P}'| = \frac{|\vec{P}| \cos \gamma - E_0}{\cos \theta_p - \sin \theta_p \frac{\sin \phi_p}{\tan \theta_e \sin \phi_e}}$$

$$\sigma_{W^2} \sim 0.2 \text{ GeV}^2$$

$$\sqrt{M^2 + 1.5\sigma_{W^2}} \simeq 1.086 \text{ GeV}$$

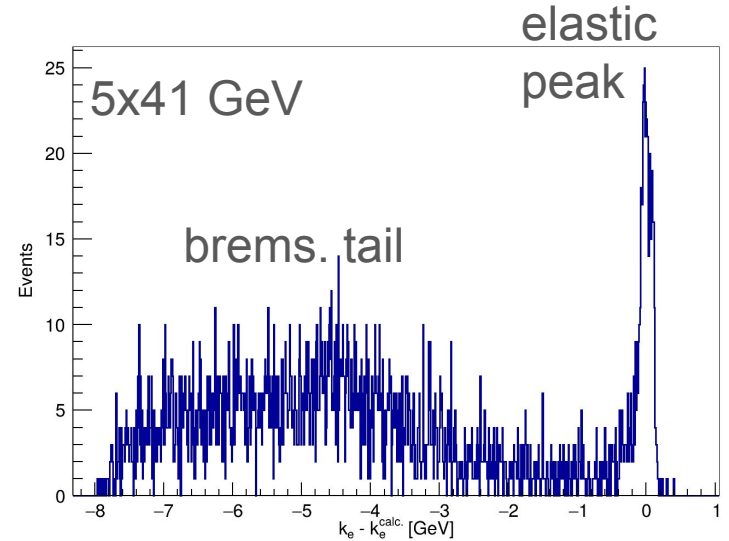
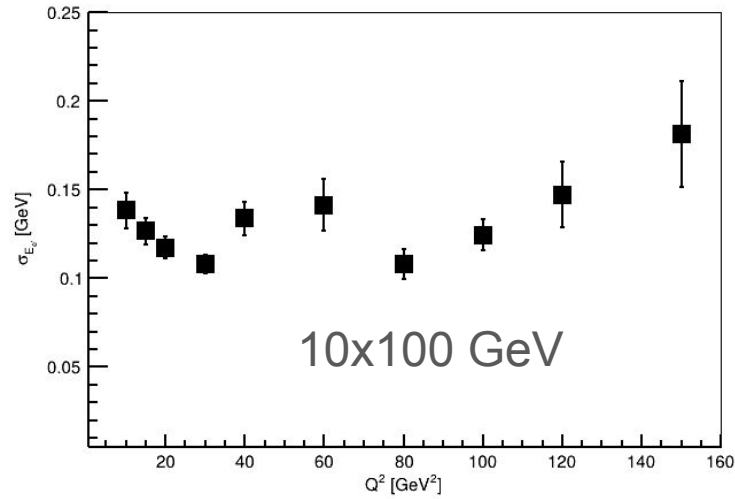


E' reconstruction

- to cut off bremsstrahlung gammas we can use LAB equations [[C. Sofiatti and T.W. Donnelly, Phys.Rev.C84, 014606 \(2011\)](#)]:

$$k' = \frac{1}{a} \left[b + E_{tot} \sqrt{\xi^2 - m_e^2 (M^2 + p_{tot}^2 \sin^2 \theta_e)} \right]$$

- comparing the measured electron momentum with calculated from the electron scattering angle allows to separate bremsstrahlung tail very clearly:



M_X^2 reconstruction

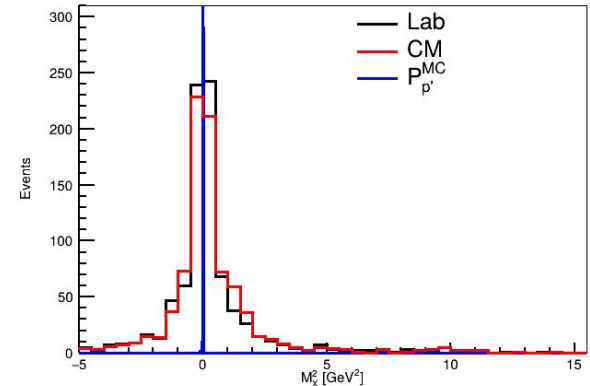
- identification of the elastic $e+p \rightarrow e'+p'$ process requires:

$$M_X^2 = \left[(k - k') + (P - P') \right]^2 < m_\pi^2$$

- no simplification is possible (until final state remains unknown);
- e-p CM can be used to cancel some spatial vectors:

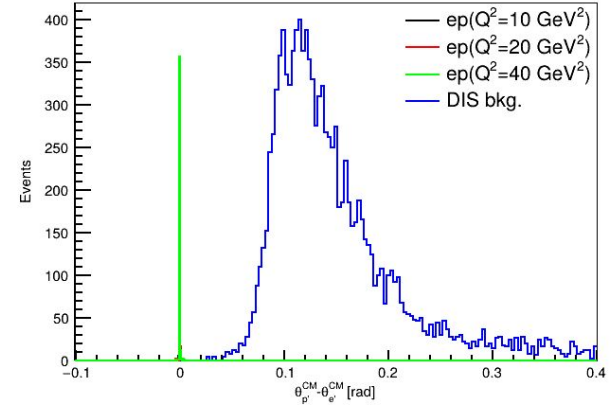
$$M_X^2 = s + M^2 + 2E_{e'}^{CM} E_{p'}^{CM} (1 - \cos \theta_{e'p'}^{CM}) - 2\sqrt{s} (E_{e'}^{CM} + E_{p'}^{CM}) < m_\pi^2$$

- no significant difference between CM and LAB;
- best resolution at 5x41 GeV and $Q^2 > 4 \text{ GeV}^2$ reaches 0.9 GeV^2 ; **NB - using generated P_p get 0.006 GeV^2 ;**
- cannot separate (3σ) channels with: $\leq 21\pi$, $\leq 6 \text{ K}$, $\leq 3 \text{ p}$;
- without AfterBurner the resolution is slightly better;
- must use 4-momentum conservation vetoes.

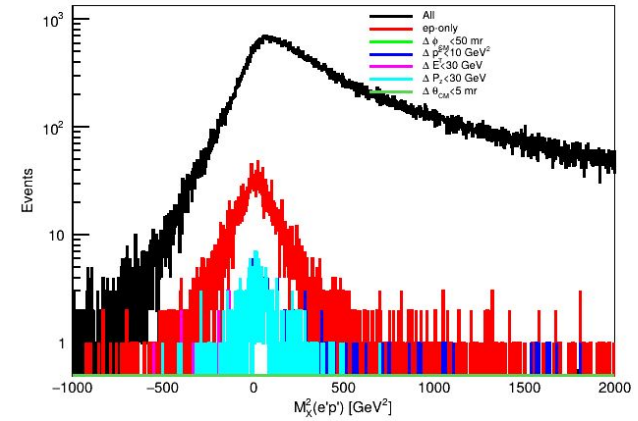
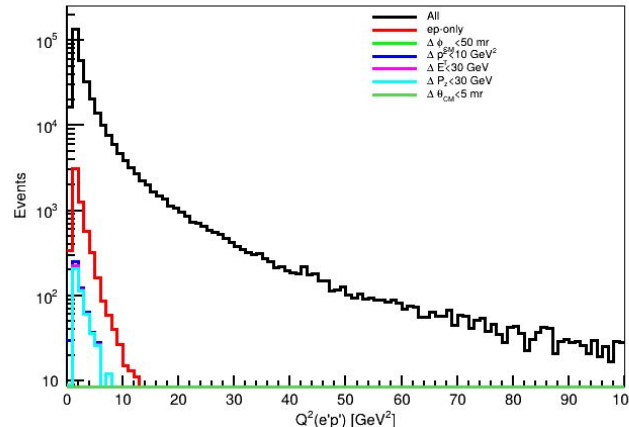
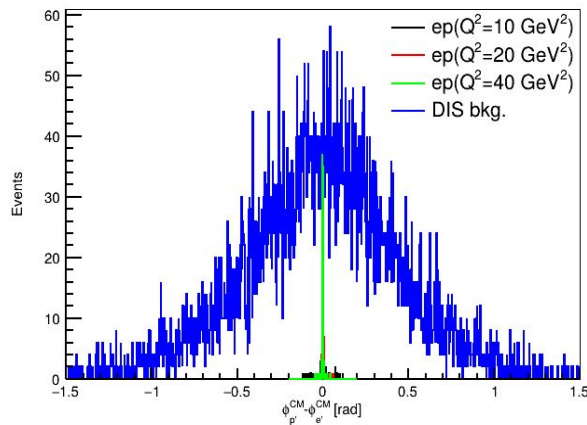


DIS backgrounds from Pythia8

1. veto on additional (to $e'p'$) reconstructed particles reduces yield by 2 orders of mag.;
2. coplanarity ($\Delta\phi$) in CM indeed provides a good elastic channel selection power;
3. P_T , E and P_z cuts have no separation power due to poor resolution;
4. the total suppression of all cuts is $0.75 \cdot 10^{-4}$, sufficient to compensate cross section ratio elastic($Q^2 > 1 \text{ GeV}^2$)/DIS($Q^2 > 1 \text{ GeV}^2$) = $2.2 \text{ nb}/0.6 \mu\text{b} = 4 \cdot 10^{-3}$;
5. Q^2 dependence of the DIS background is similar to the elastic one, background residuals are mostly present at low Q^2 and can be completely removed by $\Delta\theta$ CM cut.



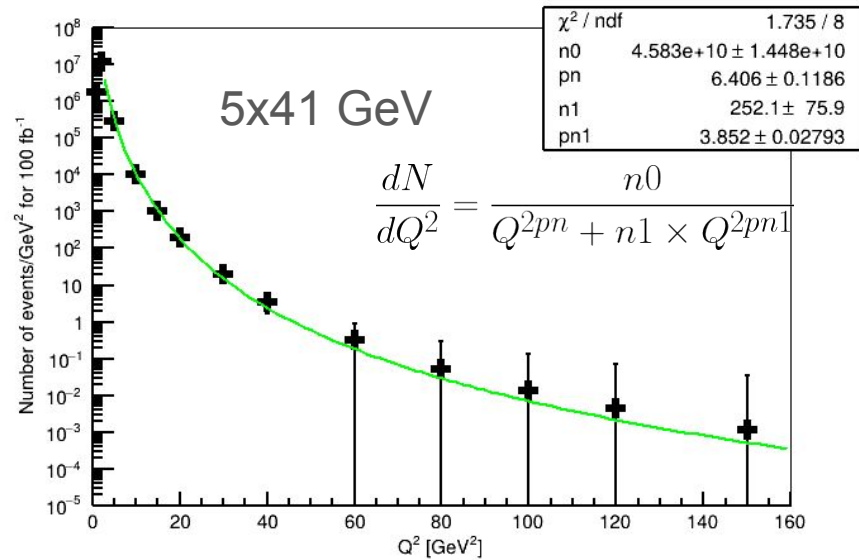
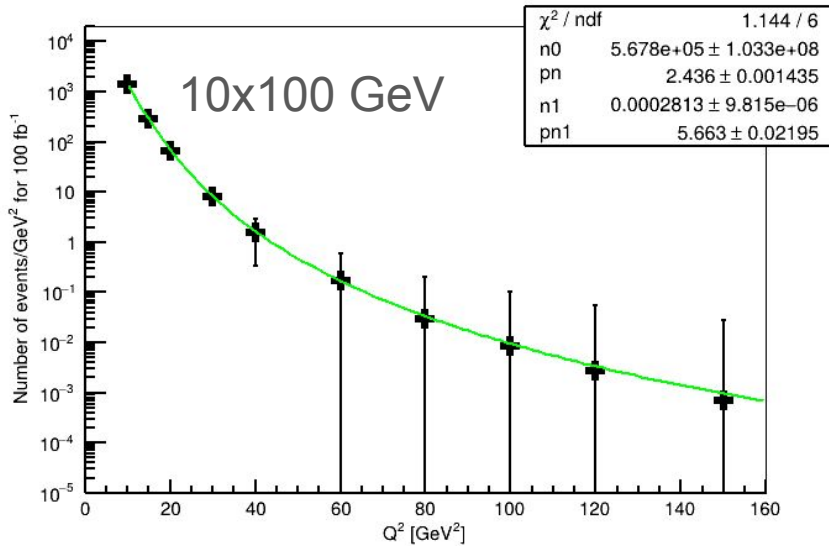
Are single pion production channels included in Pythia8?



Projected statistics

- number of events are similar to the previous study, except the low Q^2 region;
- statistical precision of 1% reached at $Q^2=10-20 \text{ GeV}^2$, for higher Q^2 elastic peak does not provide a precise reference.

$$L_{MC} = \frac{N_{gen}}{\int \sigma_{MC}(Q^2) dQ^2} \quad N_{proj} = N_{rec} \frac{L_{ePIC}}{L_{MC}} = \frac{N_{rec}}{N_{gen}} L_{ePIC} \int \sigma_{MC}(Q^2) dQ^2$$



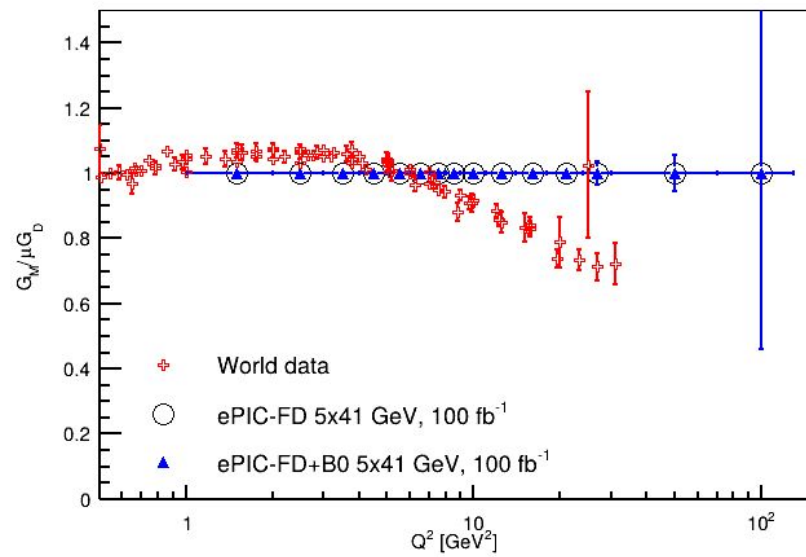
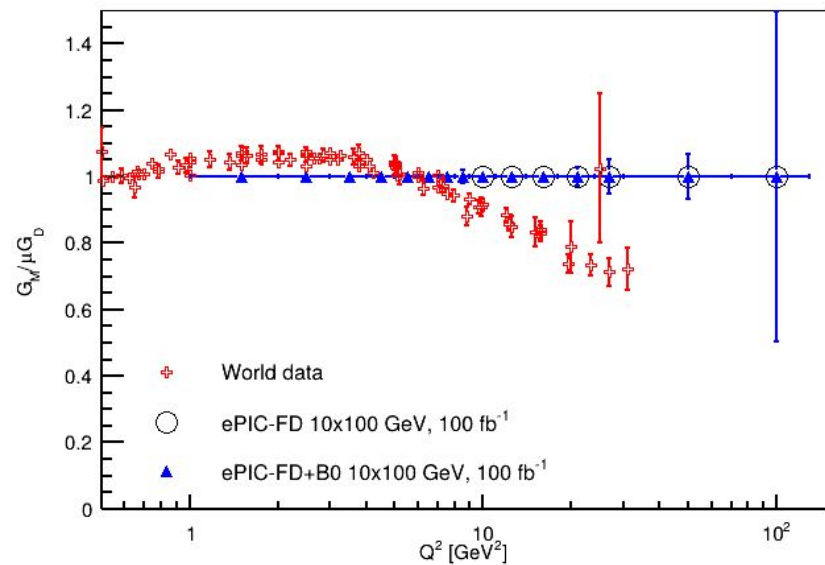
Final Runs projections

- at 100 GeV FD($\eta < 3.5$) acceptance limits $Q^2 > 10 \text{ GeV}^2$, high stat. up to 50 GeV^2 ;
- at 41 GeV FD($\eta < 3.5$) acceptance limits $Q^2 > 2 \text{ GeV}^2$, high stat. up to 50 GeV^2 ;
- at 100 GeV most of low Q^2 events are measured by B0 ($\eta > 4.6$).

$$\theta_p(E_p = 100 \text{ GeV}, Q^2 = 10 \text{ GeV}^2) \sim 1.8^\circ$$

$$\theta_p \xrightarrow{E \rightarrow \infty} \frac{\sqrt{Q^2}}{E_p}$$

$$\theta_p(E_p = 41 \text{ GeV}, Q^2 = 1 \text{ GeV}^2) \sim 1.4^\circ$$



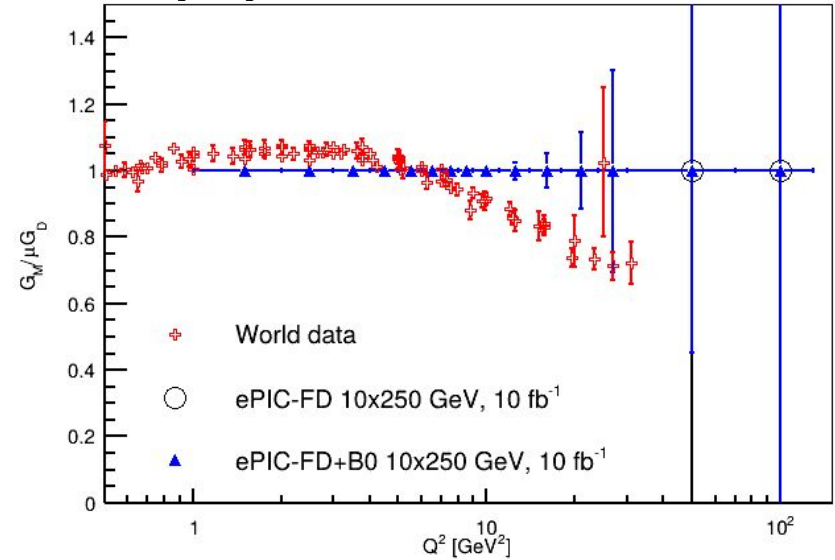
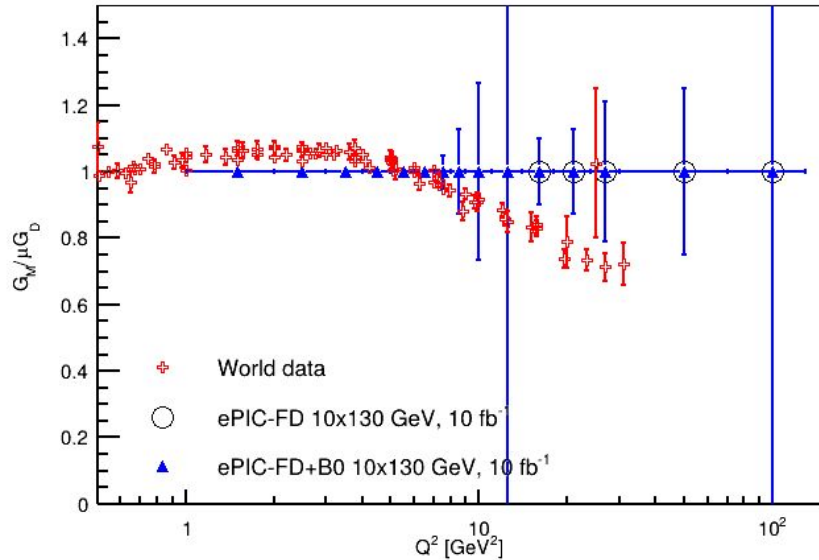
Early Physics projections

- at 130 GeV FD($\eta < 3.5$) acceptance limits $Q^2 > 15 \text{ GeV}^2$, allowing to measure 50 events;
- at 250 GeV FD($\eta < 3.5$) acceptance limits $Q^2 > 40 \text{ GeV}^2$, allowing to measure 0.2 events;
- most of low Q^2 events are measured by B0 ($\eta > 4.6$). Some lost in the gap between FD and B0.

$$\theta_p \xrightarrow{E \rightarrow \infty} \frac{\sqrt{Q^2}}{E_p}$$

$$\theta_p(E_p = 130 \text{ GeV}, Q^2 = 20 \text{ GeV}^2) \sim 2^\circ$$

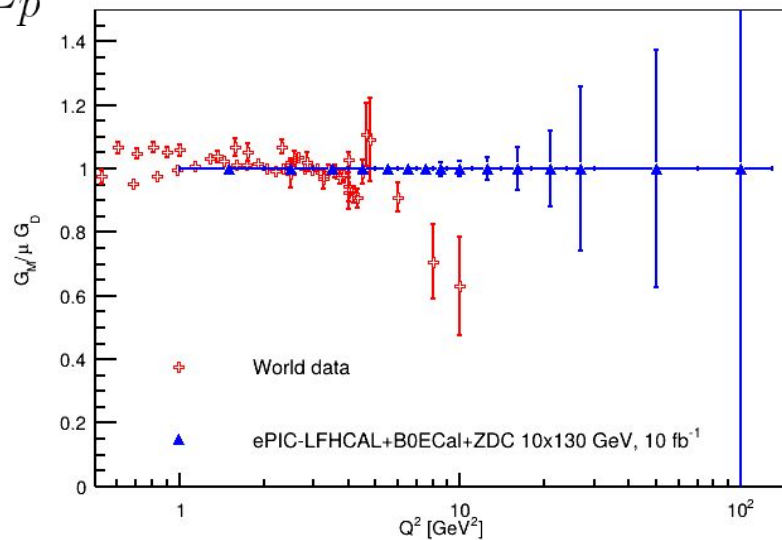
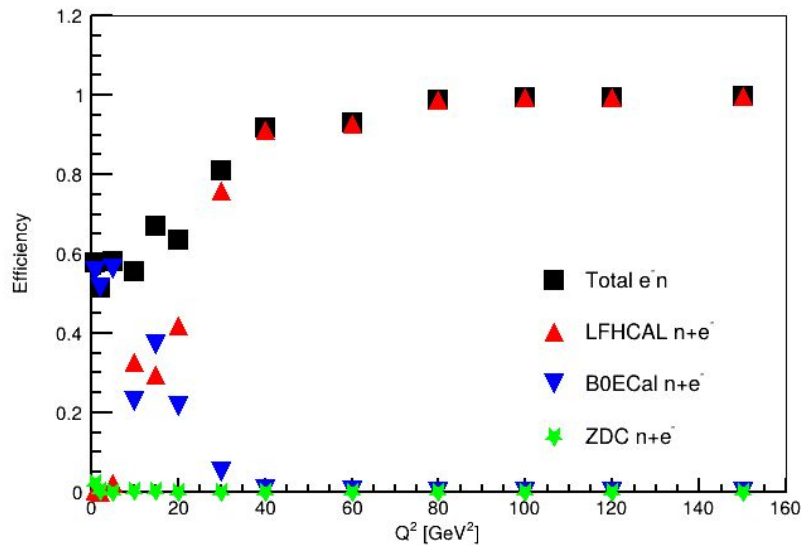
$$\theta_p(E_p = 250 \text{ GeV}, Q^2 = 40 \text{ GeV}^2) \sim 1.5^\circ$$



Early Physics projections for e-n

- e-D data at 130 GeV may allow to access less known neutron G_m ;
- selected clusters in LFHCAL, B0ECal and ZDC with deposited energy >1 MeV;
- like for the proton, at $Q^2 < 15 \text{ GeV}^2$ B0ECal is most efficient, above - LFHCAL;
- no background or [neutron PID](#) is considered here (every cluster = n).

$$\theta_p(E_p = 130 \text{ GeV}, Q^2 = 20 \text{ GeV}^2) \sim 2^\circ \quad \theta_p \xrightarrow{E \rightarrow \infty} \frac{\sqrt{Q^2}}{E_p}$$

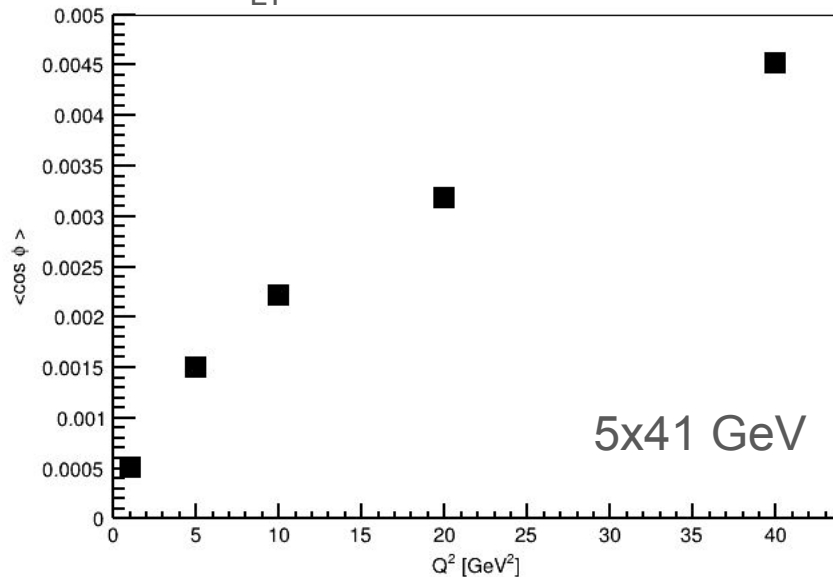
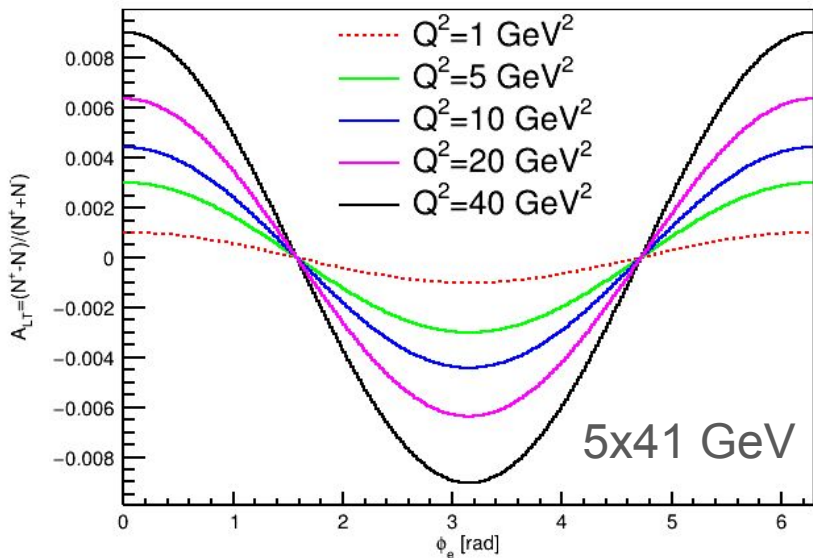


Projected proton spin asymmetries

- polarization asymmetry for transversely polarized protons indeed has $\cos(\varphi)$ shape;
- asymmetry increases with Q^2 , but the absolute value is small $<0.5\%$;
- at $Q^2=10 \text{ GeV}^2$ we expected 10^4 events/ 100 fb^{-1} , thus the error on asymmetry $>1\%$.

$$\lim_{A_{LT} \rightarrow 0} \sigma_{A_{LT}} \simeq \frac{1}{\sqrt{N_{tot}}}$$

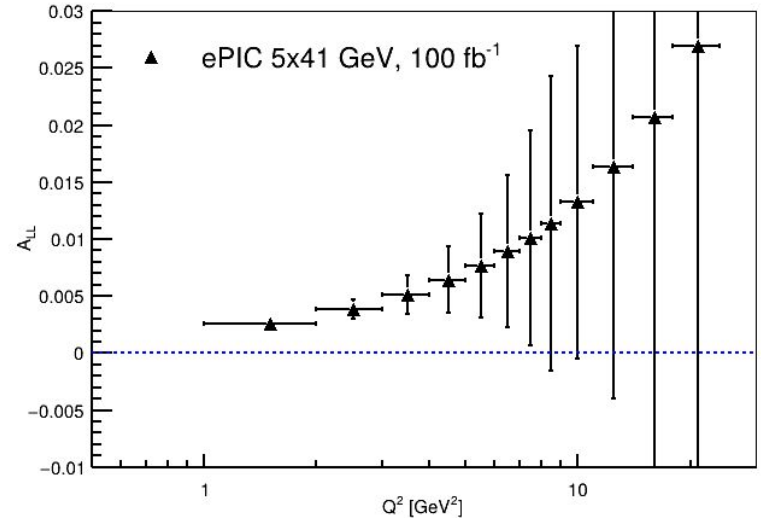
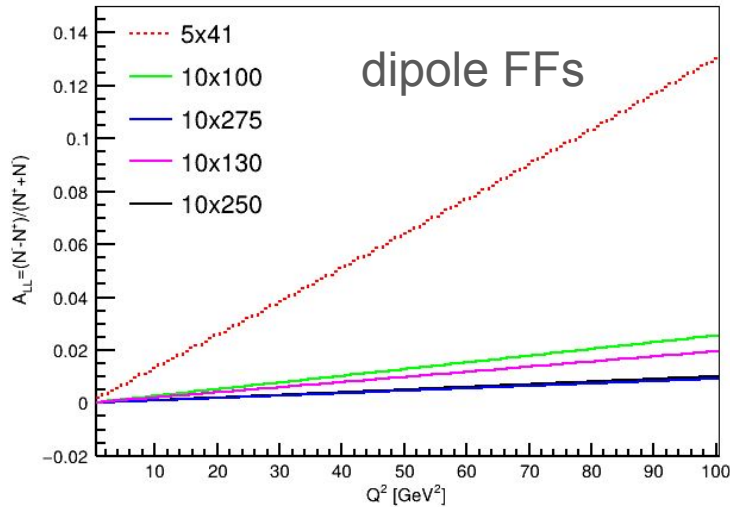
at JLab 11 GeV $Q^2=10 \text{ GeV}^2$
 A_{LT} will be 11%



Projected double spin asymmetries

- double spin asymmetry for longitudinally polarized electrons and protons increases linearly with Q^2 ;
- asymmetry is largest at lowest ePIC energy - 5x41 GeV;
- with 100 fb^{-1} the asymmetry can be measured up to $Q^2=5-7 \text{ GeV}^2$, however the precision could be insufficient to obtain G_E/G_M (maybe combining many runs it will be feasible).

$$\sigma_{A_{LL}} \xrightarrow{A_{LL} \rightarrow 0} \frac{1}{P_e P_p \sqrt{N}}$$



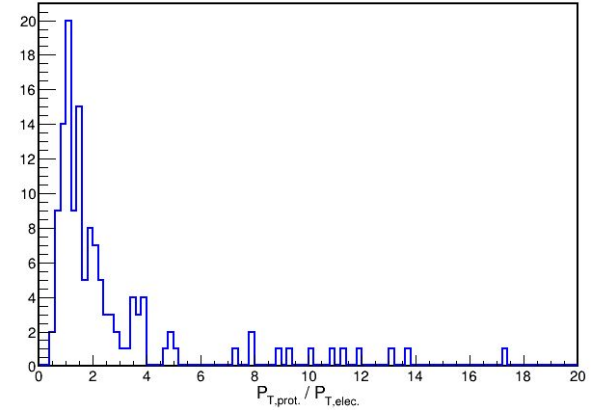
Conclusions

- elastic scattering is the most precisely (1%) known cross section in e-p scattering, which can be used at EIC as a reference for the absolute efficiency benchmark;
- overall angular resolutions are good, while momentum resolutions are much larger than pion mass scale; dRICH could improve momentum resolution for protons at lowest energy;
- e^- efficiency is high everywhere (except $Q^2 < 1 \text{ GeV}^2$), but p-efficiency of FD is suppressed at low Q^2 , where proton goes into the the gap between FD($\eta < 3.5$) and B0($\eta > 4.6$) or in B0;
- peak contribution falls exponentially with Q^2 , reaching 10^{-4} at $Q^2 = 10 \text{ GeV}^2$, requiring a high resolution on W to remove the bremsstrahlung tail;
- missing mass resolution is insufficient to isolate the elastic channel, proton momentum resolution is dominant contribution to this uncertainty, but angular correlation in CM seems to solve this problem;
- projected statistics allow to reach 1% stat. precision at $Q^2 < 10 \text{ GeV}^2$, mostly covered by B0-detector;
- polarization asymmetries may allow to measure G_E/G_M ratio, but asymmetries are small at ePIC and statistical precision might be insufficient.

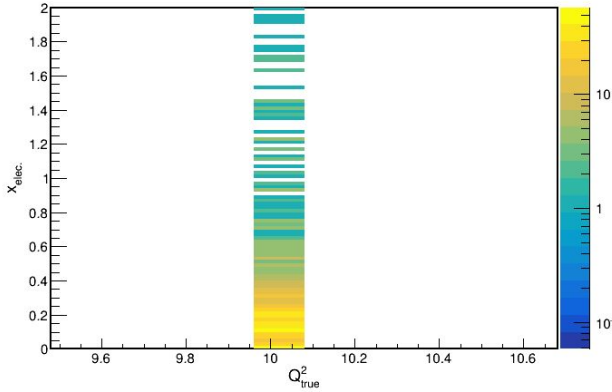
Collider kinematic methods

- using “Elastic_reco.C” macro from previous study we found that none of methods able to reconstruct x ;
- only Q^2 reconstructed by DA method is very precise, but x is offset;
- ϕ and p_T widths in LAB are 10÷100 times larger than in previous study (50 mrad \rightarrow 500 mrad, 0.05 GeV \rightarrow 5 GeV).

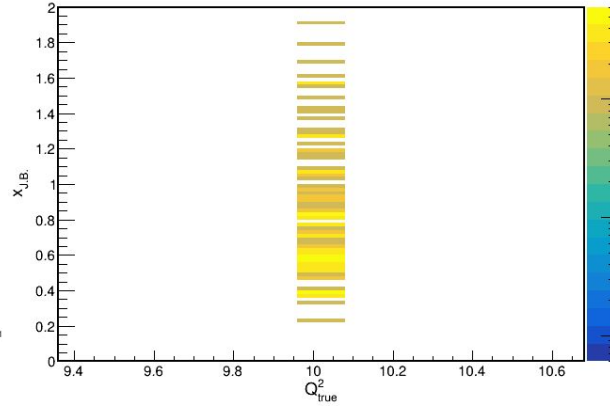
Reconstructed proton and electron P_T balance: Colinear frame



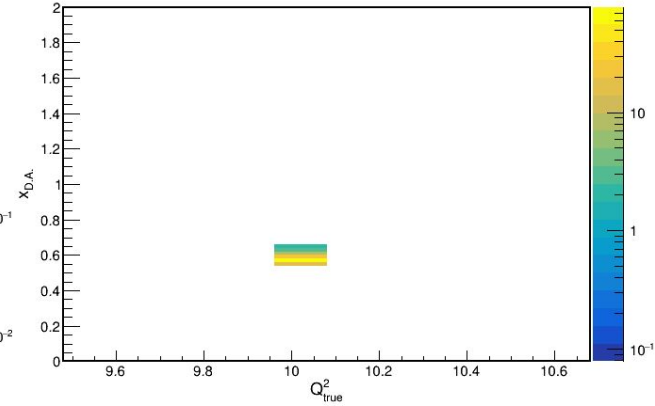
x reconstruction: electron method



x reconstruction: J.B. method



x reconstruction: D.A. method



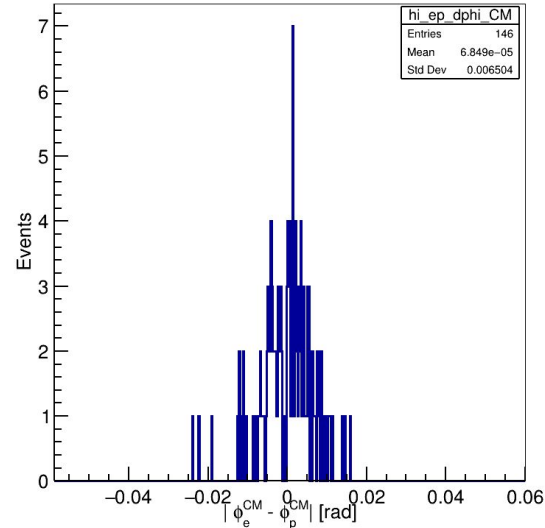
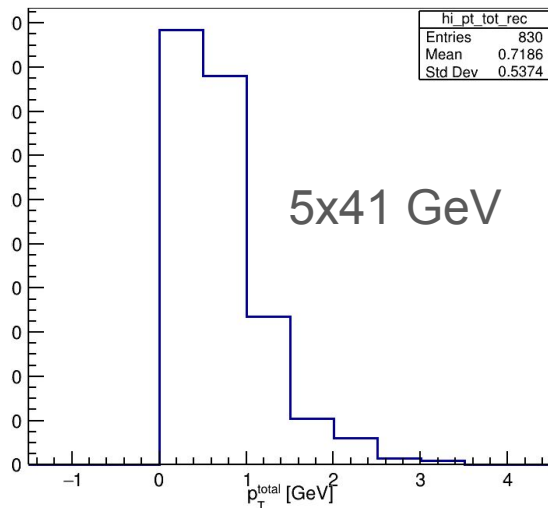
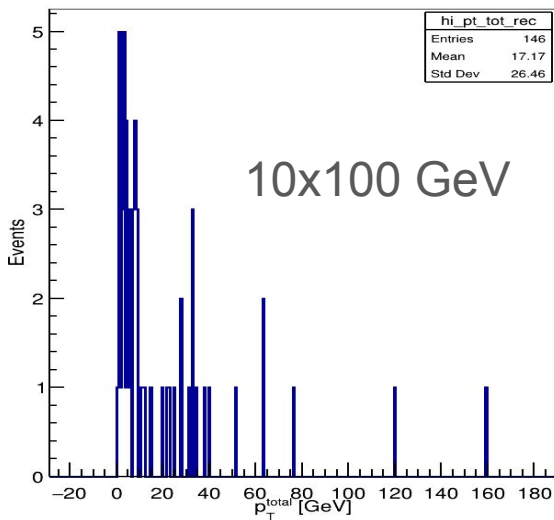
4-momentum conservation veto

- p beam is off-axis, p_T and φ balance should include crossing angle correction, or evaluated in CM:

$$\sqrt{\vec{p}_{T,e-p}^2 - \vec{p}_{T,beam}^2} = 0$$

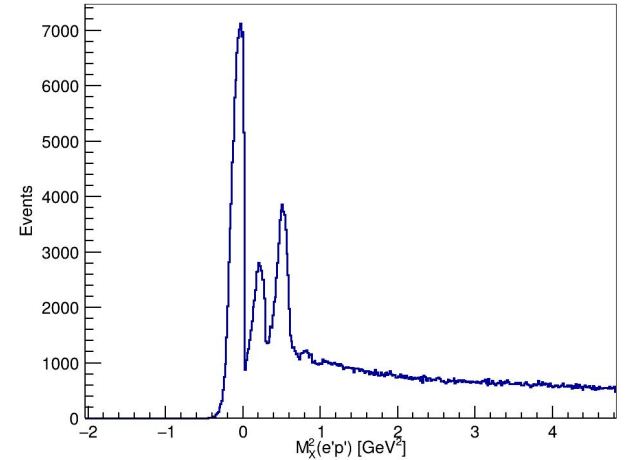
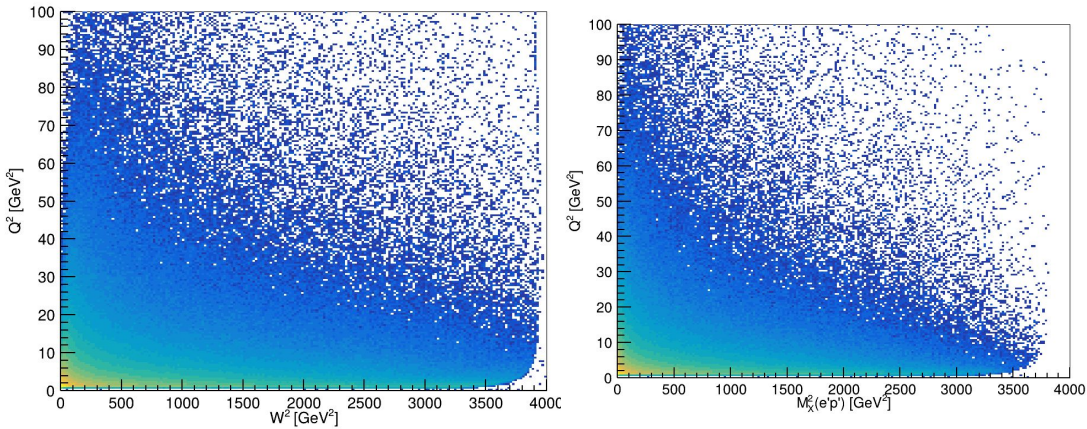
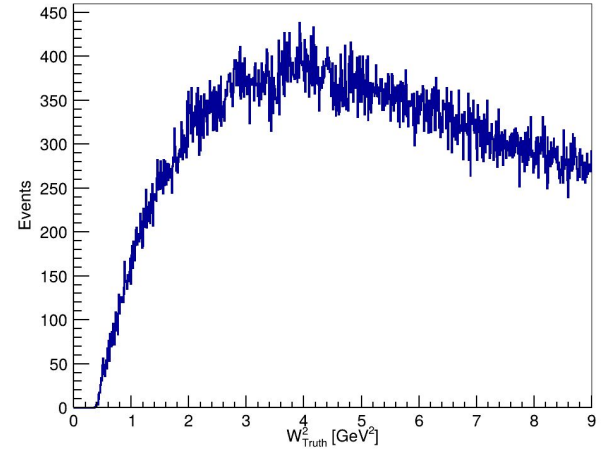
- coplanarity ($\Delta\varphi$) in CM indeed provides a good channel selection power.

$Q^2=10 \text{ GeV}^2$

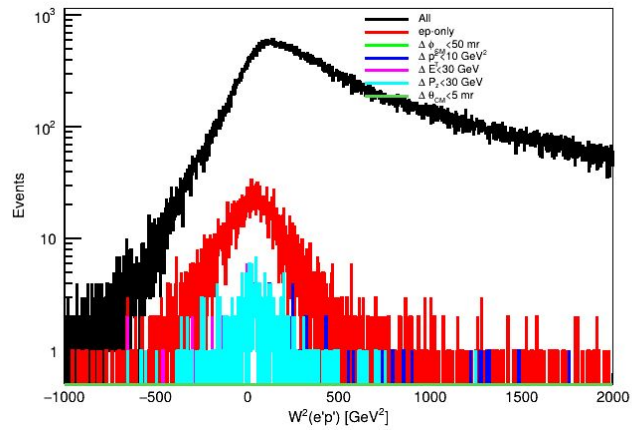
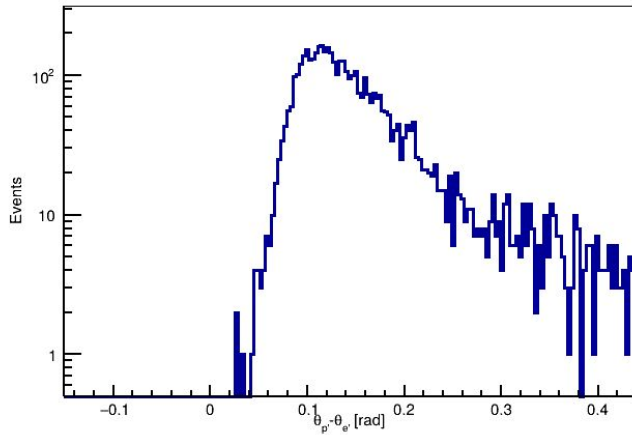
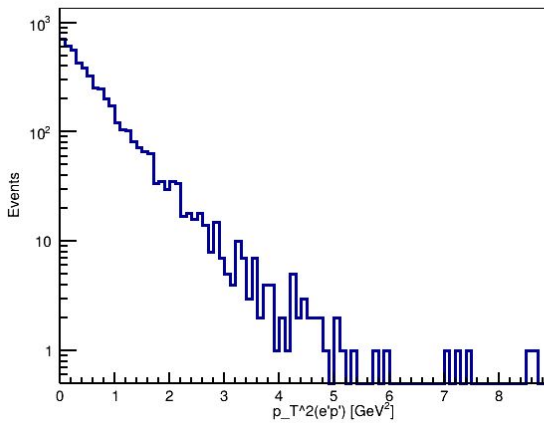
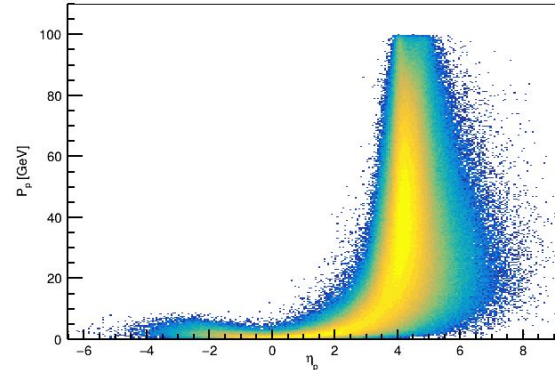
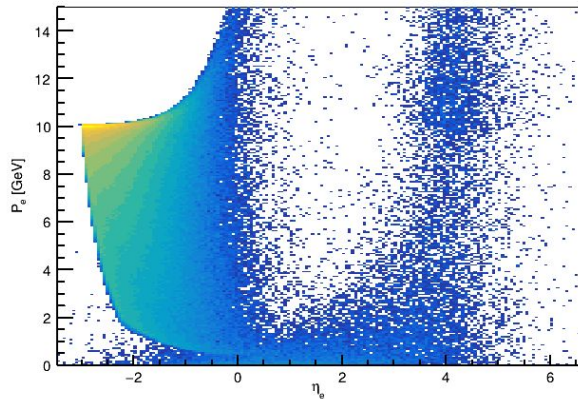
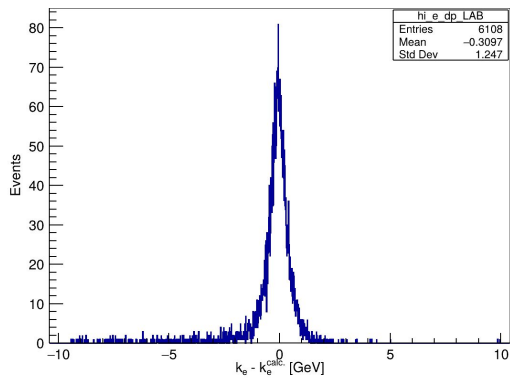


DIS backgrounds from Pythia8

1. Pythia8 simulation extends below elastic peak $W=M$, but shows no peaks of elastic and nucleon resonances;
2. it extends to zero missing mass, and exhibits 3 peaks, at -0.03 , 0.22 and 0.5 GeV^2 , presumably π^0 , η and ρ^0 ;
3. this region perhaps can be used as an estimate of elastic e'p' channel background.



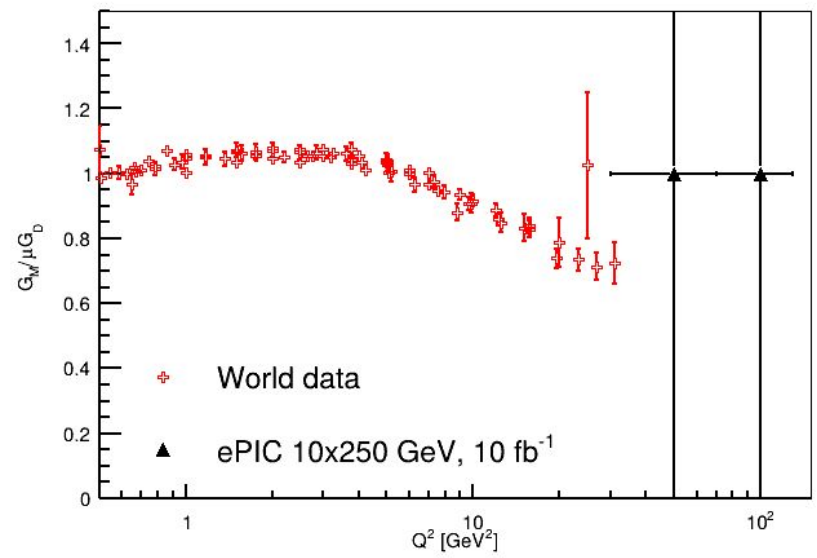
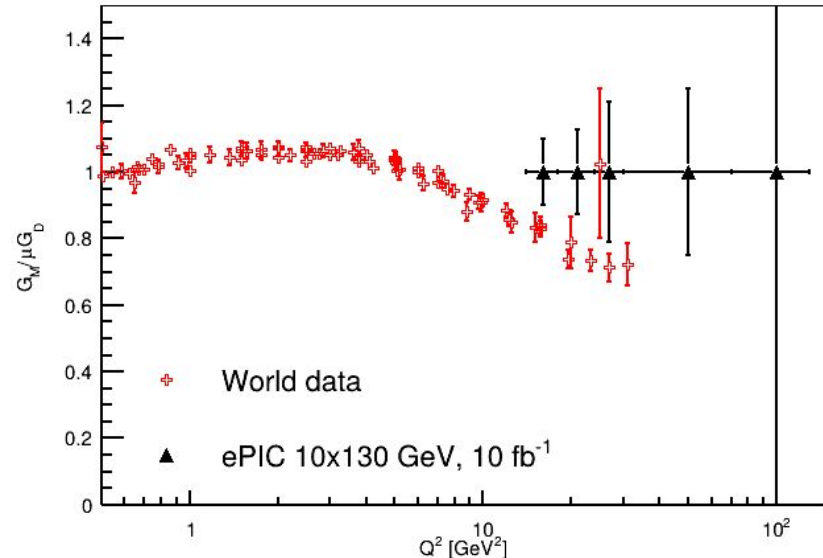
DIS backgrounds from Pythia8



Early Physics projections

- at 130 GeV FD($\eta < 3.5$) acceptance limits $Q^2 > 20 \text{ GeV}^2$, allowing to measure 50 events;
- at 250 GeV FD($\eta < 3.5$) acceptance limits $Q^2 > 40 \text{ GeV}^2$, allowing to measure 0.2 events;
- most of low Q^2 events are below FD ($\eta < 3.5$) and can be measured in B0 ($\eta > 4.6$).

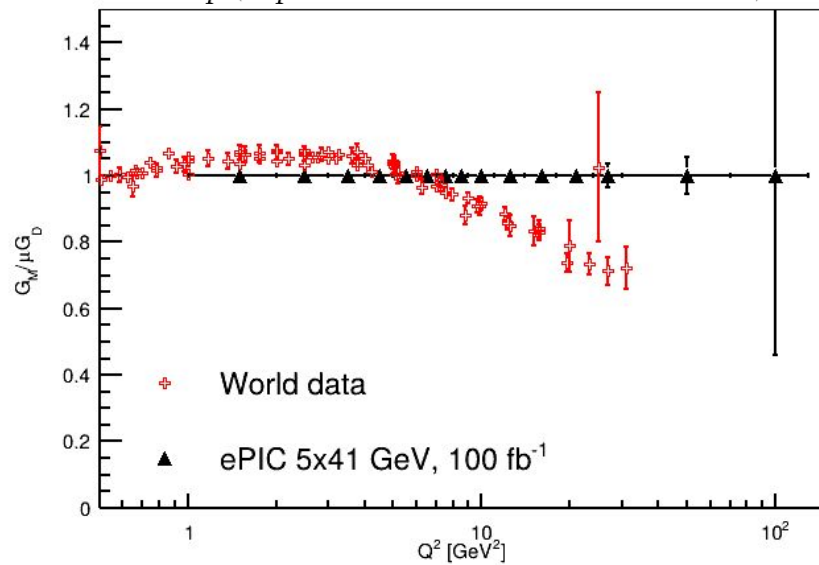
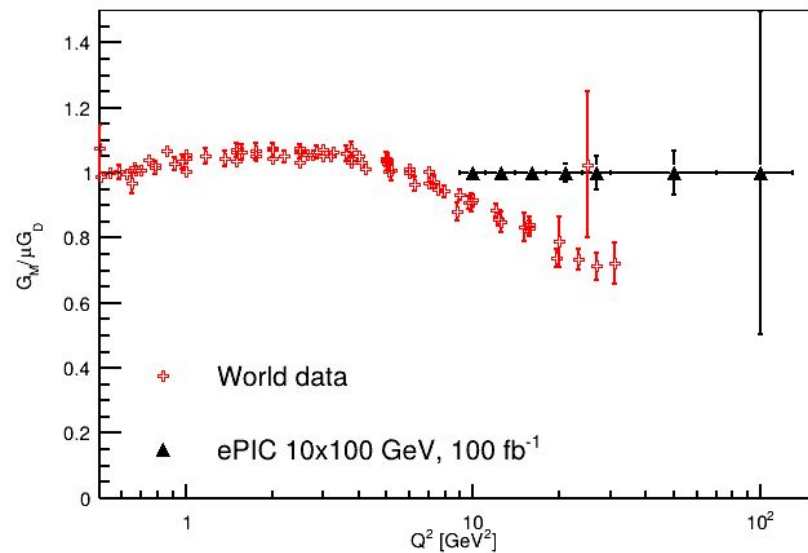
$$\theta_p(E_p = 130 \text{ GeV}, Q^2 = 20 \text{ GeV}^2) \sim 2^\circ \quad \theta_p \xrightarrow{E \rightarrow \infty} \frac{\sqrt{Q^2}}{E_p} \quad \theta_p(E_p = 250 \text{ GeV}, Q^2 = 40 \text{ GeV}^2) \sim 1.5^\circ$$



Final Runs projections

- at 100 GeV FD($\eta < 3.5$) acceptance limits $Q^2 > 10 \text{ GeV}^2$, high stat. up to 50 GeV^2 ;
- at 41 GeV FD($\eta < 3.5$) acceptance limits $Q^2 > 40 \text{ GeV}^2$, allowing to measure 0.2 events;
- low Q^2 events are detected in B0 ($\eta > 4.6$).

$$\theta_p(E_p = 100 \text{ GeV}, Q^2 = 10 \text{ GeV}^2) \sim 1.8^\circ \quad \theta_p \xrightarrow{E \rightarrow \infty} \frac{\sqrt{Q^2}}{E_p} \quad \theta_p(E_p = 41 \text{ GeV}, Q^2 = 1 \text{ GeV}^2) \sim 1.4^\circ$$



130 GeV neutron in calorimeters

